Active Contours With Area-Weighted Binary Flows For Segmenting Low SNR Imagery

Yongjian Yu and Scott T. Acton
Virginia Image and Video Analysis (VIVA), Electrical and Computer Engineering
University of Virginia, Charlottesville, VA 22903

Abstract: We investigate the detection of region boundaries in low SNR images using region based active contours. In this paper, we first show that the region based active contours models based on the region mean-difference binary flows suffer from two drawbacks when being applied to the detection of low SNR objects: (1) the contours give biased boundary locations if the image is smoothed with a linear filter; (2) the contours detect numerous false boundaries if the image is not prefiltered. Toward this end, we present a model that quantifies the contour location bias. Then, we derive a new region based model to detect the boundaries of objects in low SNR imagery, based on techniques of curve evolution, area-weighted mean-difference binary flows, and level sets. Finally, we present various experimental results to illustrate that the area-weighted technique can overcome the drawbacks of the existing method.

1. Introduction

The elemental idea behind snakes and active contours is using a curve to delineate object boundaries by first initializing a curve within the image plane and evolving the curve to fit the boundary. From the perspective of this paper, there are two kinds of active contours: the edge based contours that rely on the image gradient [3] to attract the snakes, and the region based contours that depend on statistical features [2, 7, 8]. Region based contours excel over the edge based versions in cases where the image noise precludes movement of the edge based contour. Furthermore, region based contours are less likely to be sensitive to the initialization of the contour.

Some important imaging modalities such as ultrasound and radar inherently generate low signal-to-noise ratio (SNR) imagery. As such, automatic segmentation of low SNR imagery represents an important category of segmentation problems. So, we investigate region based contours for the segmentation of low SNR imagery, as edge based active contours and edge detection itself often fails in instances of low SNR. We first scrutinize mean-difference binary-flow models and discuss shortcomings. Then, we propose a modification to the model that reduces edge location bias and false positive edges. Finally, we provide examples of experimental results and compare the results obtained with the area-weighted approach with those yielded by the existing mean-difference model. Quantitative as well as qualitative measures of success are given.

1.1. Mean-Difference Binary Flows

With a binary flow, we assume that the image domain Ω is divided into two regions $\{R, R_c\}$ bordered by a closed curve $\vec{C}$. Yezzi *et al.* [7] derived an innovative class of region based active contours for global segmentation of bimodal imagery by minimizing the following cost functional

$$E = -\frac{\lambda}{2}(u-v)^2 + \mu\int_{\vec{C}} ds, \qquad (1)$$

where u and v are the arithmetic means of the image signal intensities I inside and outside the curve $\vec{C}$, respectively. A_u and A_v are the corresponding areas of region R and region R_c. λ and μ are weighting parameters. The contour that minimizes (1) can be found by solving

$$\vec{C}_t = \lambda(u-v)\left[\frac{I-u}{A_u} + \frac{I-v}{A_v}\right]\vec{N} - \mu\kappa\vec{N}, \qquad (2)$$

where κ denotes the signed curvature of curve $\vec{C}$ and $\vec{N}$ is the outward normal to $\vec{C}$.

The curve evolution equation (2) is implemented numerically with the help of the level set methods of Osher [4]. Formulating the curve $\vec{C}$ as the zero level set of a Lipschitz function $\phi : \Omega \to R$, such that ϕ is positive inside $\vec{C}$ and negative outside $\vec{C}$, it can be shown [4] that solving (2) is equivalent to solving

$$\phi_t = |\nabla\phi|\left\{\mu\nabla\cdot\left(\frac{\nabla\phi}{|\nabla\phi|}\right) + \lambda(u-v)\left[\frac{I-u}{A_u} + \frac{I-v}{A_v}\right]\right\}. \qquad (3)$$

The zero-crossings of ϕ reveal the curve position. Note that in (3), the image I is defined only on the zero level set of the function ϕ. To solve (3), therefore, the values of the image I on other level sets need to be found through the speed extension process [6]. Usually, the value of I at a point (x, y) away from the zero level set is set to that of the closest point within the zero level set.

The speed extension is computationally expensive. In our implementation of (3), we adopt the narrow band technique of [2] for the speed extension, resulting in the following level set formulation:

0-7803-7750-8/03/$17.00 ©2003 IEEE

$$\phi_t = \delta_\varepsilon(\phi)|\nabla\phi|\left\{\mu\nabla\cdot\left(\frac{\nabla\phi}{|\nabla\phi|}\right)+\lambda(u-v)\left[\frac{I-u}{A_u}+\frac{I-v}{A_v}\right]\right\}, \quad (4)$$

where $u=(1/A_u)\iint_\Omega I(x,y)H_\varepsilon(\phi(x,y))dxdy$,

$v=(1/A_v)\iint_\Omega I(x,y)[1-H_\varepsilon(\phi(x,y))]dxdy$,

$A_u=\iint_\Omega H_\varepsilon(\phi(x,y))dxdy$,

$A_v=\iint_\Omega[1-H_\varepsilon(\phi(x,y))]dxdy$,

$H_\varepsilon(z)=\frac{1}{2}\left[1+\frac{2}{\pi}\arctan\left(\frac{z}{\varepsilon}\right)\right]$, $\delta_\varepsilon(z)=dH_\varepsilon(z)/dz$, and ε is a regularization parameter.

With (4), the value of I on any point (x, y) is simply the intensity of the image on that point. In the numerical implementation, the spatial derivatives for calculating the curvature are computed via a central differencing scheme.

1.2. Experimental Observation

Here we provide an experiment to show that the contour extracted by (4) is biased in location when the SNR of an object is low and prefiltering of image is applied. For this purpose, we use a 256 by 256 synthetic image shown in Fig.1 (a). The image is formed by first setting the image value in the bright region to be I_1=0.4 and that in the dark regions to be I_2=0; and then by adding Gaussian noise of zero mean and variance σ^2=0.3 to the image. Defining the signal-to-noise ratio by $\mathrm{SNR}=10\log_{10}\left[(I_1-I_2)^2/\sigma^2\right]$, this example image has an SNR of 1.26dB. We observed that directly applying the active contour model of (3) or (4) to Fig.1 (a) results in highly irregular contours containing numerous artifacts such small blobs, and that the correct boundary could not be extracted by simply increasing the weight of the curvature term. We also observed that applying (3) or (4) to a Gaussian smoothed image yields improved segmentation: the extracted contour becomes smoothed and interior holes disappear. Fig. 1(b) shows the segmentation result of Fig.1(a) by applying (4) to a Gaussian filtered image $\tilde{I}(x,y)=I(x,y)*G_4(x,y)$ where $G_4(x,y)$ is a Gaussian kernel with standard deviation of 4. In Fig. 1(b), the contour location bias of the mean-difference method is illustrated.

1.3. An Interpretation of the Location Bias

Is there any analytical evidence that supports the existence of location bias for the mean-difference method? To answer this question, we propose a model to interpret the experimental results observed and derive an approximated expression of the bias. Consider a step edge image contaminated by a Gaussian white noise:

$$I(x,y)=I_1+(I_2-I_1)u(x)+n, \quad (5)$$

where $u(x)$ is a 1-D unit step function; $n\sim N(0,\sigma^2)$, and constants I_1 and I_2 are the mean intensity values of the bright side and dark side of the image. Fig.2. illustrates the two-region model image. Let L be the height of the image, W_1 and W_2 be the widths of the dark region and bright region, respectively. The broken line indicates the resulted segmenting curve $\vec{C}$. Convolving (5) with a 2-D Gaussian kernel of standard deviation α, we obtain a smoothed version of (5):

$$\tilde{I}(x,y)=\frac{I_2+I_1}{2}+\frac{I_2-I_1}{2}erf\left(\frac{x}{\alpha}\right)+\tilde{n}, \quad (6)$$

where $erf(x)$ is error function and $\tilde{n}\sim N(0,\tilde{\sigma}^2)$ with $\tilde{\sigma}=\sigma/(2\sqrt{\pi}\alpha)$.

When the active contour of (3) is evolved on (6) and converged, the following equilibrium equation should be satisfied

$$\left\{\mu\kappa+\lambda(u-v)\left[\frac{\tilde{I}-u}{A_u}+\frac{\tilde{I}-v}{A_v}\right]\right\}=0. \quad (7)$$

Assuming that the evolving curve $\vec{C}$ converges to a straight line $x=x_0$, located close to the true boundary (*i.e.*, the y axis), we have that the curvature κ = 0. If the regularization parameter ε is larger than the scale of the edge α, we have that $u\cong I_1$, $v\cong I_2$, $A_u\cong(W_1+x_0-\varepsilon)\cdot L$ and $A_v\cong(W_2-x_0-\varepsilon)\cdot L$.

With the approximation $erf(x)\approx\frac{2x}{\sqrt{\pi}}$ for $|x|<<1$, we can write that $\tilde{I}(x_0)\cong\frac{I_1+I_2}{2}+\frac{I_2-I_1}{\sqrt{\pi}\alpha}x_0+\tilde{n}$.

Neglecting the sufficiently suppressed noise term in $\tilde{I}(x_0)$ and substituting all needed quantities into (7) yields

$$\frac{1/2+x_0/(\sqrt{\pi}\alpha)}{W_1+x_0-\varepsilon}+\frac{-1/2+x_0/(\sqrt{\pi}\alpha)}{W_2-x_0-\varepsilon}=0. \quad (8)$$

Solving (8) gives the estimated contour location bias:

$$x_0\cong\frac{W_2-W_1}{2-2(W_2+W_1-2\varepsilon)/(\sqrt{\pi}\alpha)}. \quad (9)$$

From (9), it is seen that the bias of the contour location is approximately proportional to the scale parameter of the filter (α) and the area-weighted contrast of the object ($\approx\frac{(W_2-W_1)L}{(W_2+W_1)L}$) since $W_1+W_2>>\varepsilon$ and $W_1+W_2>2$.

2. The Area-Weighted Method

In some region merging based segmentation algorithms such as [1], the dissimilarity metrics used in

merging are weighted by the sizes of the regions. Comparing the first term in (1) with the dissimilarity metric in such region-merging-based segmentation, we propose that the bias of the mean-difference method can be eliminated by modifying (1) as

$$E = -\frac{\lambda}{2}\frac{A_u A_v}{A}(u-v)^2 + \mu\int_C ds, \qquad (10)$$

where A is the size of the image. The contour minimizing (10) can be found via the following curve evolution equation

$$\vec{C}_t = \frac{\lambda}{A}(u-v)\left[A_v(I-u)+A_u(I-v)-(1/2)(A_u-A_v)(u-v)\right]\vec{N} - \mu\kappa\vec{N}. \qquad (11)$$

An equivalent level set formulation of (11) is given by

$$\phi_t = \delta_\varepsilon(\phi)|\nabla\phi|\left\{\mu\nabla\cdot\left(\frac{\nabla\phi}{|\nabla\phi|}\right)+\frac{\lambda}{A}(u-v)\left[A_v(I-u)+A_u(I-v)-\frac{1}{2}(A_u-A_v)(u-v)\right]\right\}, \qquad (12)$$

Using the same approach used with deriving (9), we have evaluated the contour location bias with (12). The contour equilibrium position equation is given by

$$(W_2-x_0-\varepsilon)(\tilde{I}(x_0)-I_1)+(W_1+x_0-\varepsilon)(\tilde{I}(x_0)-I_2) - \frac{1}{2}(W_1-W_2+2x_0)(I_1-I_2)=0. \qquad (13)$$

From (13) we find that $x_0 = 0$. Therefore, the area-weighted model for active contours yields an unbiased contour location no matter how much the image has been smoothed and regardless of the foreground/background size. Fig. 1(c) shows the segmentation result from Fig. 1(a) obtained by applying (12) to the smoothed image $\tilde{I}(x,y) = I(x,y) * G_4(x,y)$.

3. Experimental Results

In this section, we first present a quantitative comparison of the mean-difference model and the area-weighted model as applied to the images of a circular object. The size of these images is 256x256 pixels. Pratt's figure of merit [5] is used to measure the edge location accuracy. For the mean-difference model, we choose the model parameters as: λ=1, μ=1, ε=1, and Δt = 0.1. For the area-weighted model, we choose $\lambda = A$ (where A is the size of the image), μ=1, ε=1, and Δt = 0.0001. The results are summarized in Table 1. These results are qualitatively in agreement with our analysis of contour location bias. Then we show several examples of the segmentation results of the area-weighted active contour algorithm as applied to synthetic and real imagery. The SNR of the synthetic image is 1.26 dB. For these two examples, the Gaussian kernel parameter α is 3.5. Fig. 3 and Fig. 4 give the corresponding segmentation results, which show qualitatively the improvements of the area-weighted model. Notice that the false edges shown in Fig. 3(b) are avoided in the area-weighted results of Fig. 3(c). The difficult segmentation of the prostate from ultrasound imagery is also improved using the area-weighted method as shown in Fig. 4.

4. Conclusions

In this paper, we evaluated the performance of a region based active contour based on mean-difference binary flows for segmenting low SNR bimodal imagery. We have shown that the boundary localization is biased when the image is smoothed. For the existing mean-difference model, we derived an expression of the bias and explained why the bias occurs. Based on this observation, we proposed a new active contour model that exploits both radiometric and area features of regions for segmenting low SNR objects in digital imagery. We compared the performance of the area-weighted algorithm with that of the binary flows, showing that the superiority of edge localization and the reduction of false edges.

References

[1] J. Beaulie, and M. Goldberg, "Hierarchy in picture segmentation: a stepwise optimization approach," *IEEE Trans. PAMI*, vol. 11, pp.150-163, 1989.

[2] T. F. Chan and L. Vese, "Active contours without edges," *IEEE Trans. on Image Processing*, vol. 10, pp. 266-277, 2001.

[3] M. Kass, A. Witkin, and D.Terzopoulos, "Snakes: active contour models," *Int. J. Comput. Vis.*, vol. 1, pp. 321-331, 1988.

[4] S. Osher, "Riemann solvers, the entropy condition, and difference approximations," *SIAM J. Numer. Anal.*, vol. 21, pp. 217-235, 1984.

[5] W. K. Pratt, *Digital Image Processing*, New York, U.S.A.: Wiley, 1977.

[6] A. Yezzi, S. Kichenassamy, A. Kumar, P. Olver, A. Tannenbaum, "A geometric snake model for segmentation of medical imagery," *IEEE Trans. Med. Imag.*, vol. 16, pp. 199-209, 1997.

[7] A. Yezzi, J. A. Tsai and A. Willsky, "A statistical approach to snakes for bimodal and trimodal imagery," *Proceedings of ICCV*, pp. 898-903, September, 1999.

[8] S. C. Zhu and A. Yuille, "Region competition: unifying snakes, region growing, and Bayes/MDL for multiband image segmentation," *IEEE Trans. PAMI*, vol. 18, pp. 884-900, 1996.

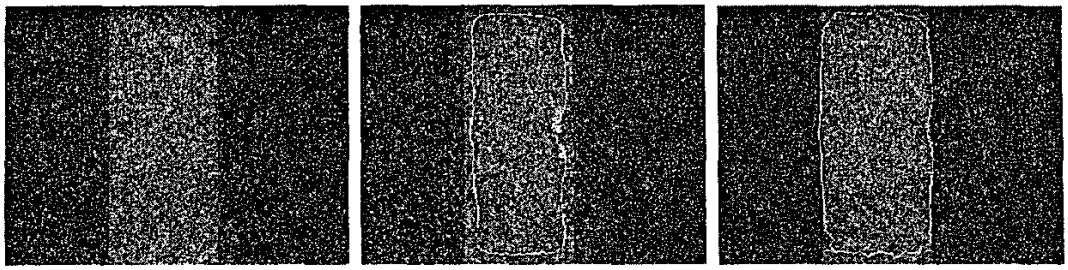

(a) (b) (c)

Fig.1. (a) Low SNR image (SNR=1.26 dB). (b) Segmentation with mean-difference model. (c) Segmentation with the area-weighted model.

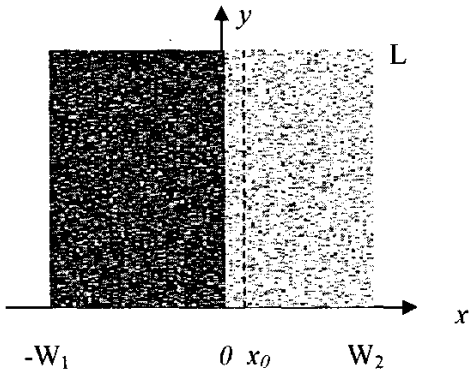

Fig.2. Noisy two-region image model used for the estimation of the contour location bias.

Table I. Pratt's Figure of Merit

SNR (dB)	α (filter scale)	FOM (Mean-Difference)	FOM (Area-Weighted)
1.25	10	0.10	0.70
6	10	0.09	0.73
16	10	0.08	0.79
1.25	4	0.27	0.85
6	4	0.49	0.89
16	4	0.52	0.89
1.25	1	0.15	0.22
6	1	0.15	0.47
16	1	0.58	0.91

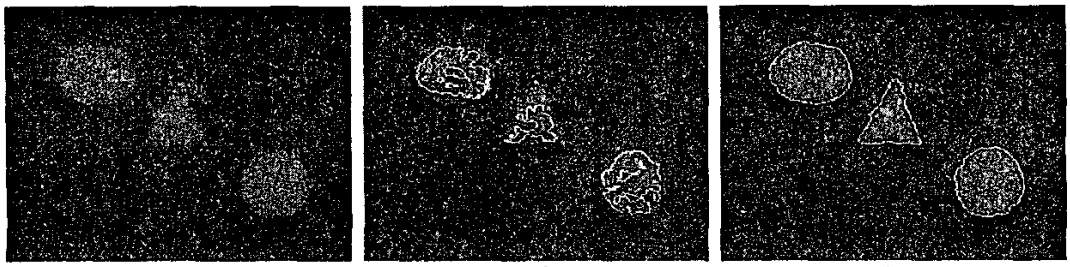

(a) (b) (c)

Fig.3. (a) Low SNR synthetic image of multiple shapes (SNR=1.26 dB). (b) Segmentation by mean-difference model. (c) Segmentation obtained with the area-weighted active contour model.

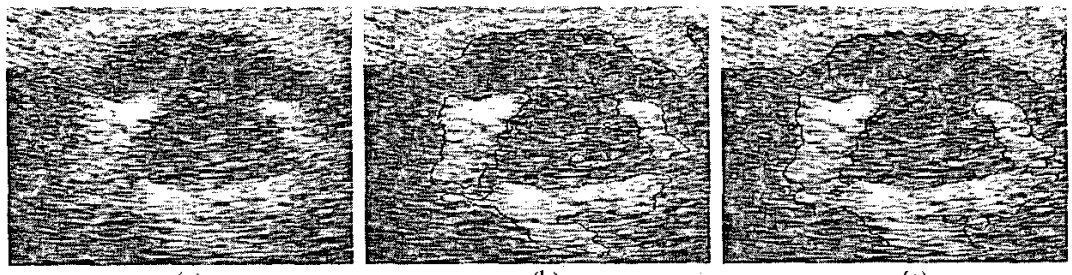

(a) (b) (c)

Fig.4. (a) Ultrasound image of prostate (log-compressed data). (b) Contour obtained with mean-difference model. (c) Contours obtained with the area-weighted model.